

# CoRoT-TESS eclipsing binaries with light-travel-time effect

T. Hajdu<sup>1,2,3,4</sup>, B. Matécsa<sup>3</sup>, J. M. Sallai<sup>3</sup> and A. Bódi<sup>1,2,4</sup>

<sup>1</sup>Konkoly Observatory, Research Centre for Astronomy and Earth Sciences (ELKH), H-1121 Budapest, Konkoly Thege Miklós út 15-17, Hungary

<sup>2</sup>CSFK, MTA Centre of Excellence, H-1121 Budapest, Konkoly Thege Miklós út 15-17, Hungary

<sup>3</sup>Eötvös Loránd University, Department of Astronomy, H-1118 Pázmány Péter stny. 1/A, Budapest, Hungary

<sup>4</sup>MTA CSFK Lendület Near-Field Cosmology Research Group, H-1121, Budapest, Konkoly Thege Miklós út 15-17, Hungary

Accepted XXX. Received YYY; in original form ZZZ

## ABSTRACT

Identifying long-period eclipsing binaries with space-based photometry is still a challenge even in the century of space telescopes due to the relatively short observation sequences and short lifetime of these missions. The Transiting Exoplanet Survey Satellite (TESS) space telescope is an appropriate tool to supplement previous space-based observations. In this paper we report the first results of the eclipse timing variation (ETV) analyses of eclipsing binaries (EBs) measured by CoRoT and TESS space telescopes. Among the 1428 EB candidates we found 4 new potential triple candidates, for which ETV was analysed and fitted by the well-known light-travel-time effect (LTTE). One of them shows significant phase shift in its folded light curve which required extra care. In this paper we also present some other systems showing significant ETV signals that could be explained by mass transfer or apsidal motion.

**Key words:** binaries: eclipsing – binaries: close – methods: numerical

## 1 INTRODUCTION

A large fraction of the detectable period changes observed in binary stars is caused by a third body, forming a gravitationally bound triple system. The evolution of these hierarchical systems can lead to the formation of exotic systems such as blue stragglers (Naoz & Fabrycky 2014) or binary neutron stars (Shappee & Thompson 2013). Thus, there is no question that the study of triple systems is important to better understand the evolution of stars in stellar systems.

In the last decade, the discovery of triple stellar systems has become relatively easy thanks to the space-based photometry of *Kepler* (Conroy et al. 2014; Borkovits et al. 2015, 2016) and TESS (Mityan et al. 2020, 2021; Rappaport et al. 2022) space telescopes. While some of these systems were discovered due to the extra eclipses of the third body, the majority were detected by eclipse timing variation (ETV). Typically, the period of the outer orbit ranges from about a few months to several years. Nowadays, thanks to continuous and precise photometry, even really compact systems with periods less than a year have become easy to identify. In addition, the combination of these observations taken at different times is also promising for discovering longer outer period systems ( $P_2 \sim$  few years).

The first space-based telescope to collect long continuous, well-sampled, high-precision photometry for a large number of stars was CoRoT, whose data formed the basis of many pioneering works (Lanza et al. 2009; Léger et al. 2009; Alencar et al. 2010; Chiappini et al. 2015; McGinnis et al. 2015). CoRoT, similar to the *Kepler* space telescope, observed thousands of eclipsing binaries, of which a comprehensive study has not yet been conducted. Only a single study was based on CoRoT measurements that identified a few close hierarchical multiple systems (Hajdu et al. 2017). Unfortunately, due to the relatively short observation sequences, the generated ETVs alone are typically not suitable for finding multi-

ples. However, based on the comprehensive analyses of the *Kepler* triples (Borkovits et al. 2016), there must be many more multiple system candidates but with longer outer periods. To find these systems the TESS space telescope can help thanks to its short but recurrent observations.

In this paper we present the first ETV analyses of binaries observed by both CoRoT and TESS space telescopes (Auvergne et al. 2009; Ricker et al. 2015). This is also the first time when we are able to identify such long (several years) period triple systems with the analyses of space telescopes measurements that cannot be discovery using only one observation sequence.

This paper is structured as follows. We formulate the basic mathematical background of the third-body affected ETV analysis in Section 2. In Section 3, we outline the steps of our study, from selecting the systems and data preparation to determining the orbital parameters of the candidates. The results of the ETV analysis are discussed in Section 4, where we also present some other systems with significant ETVs. Finally, a short summary is given in Section 5.

## 2 LIGHT-TRAVEL-TIME EFFECT

The analysis of hierarchical triple stellar systems plays a significant role in the understanding of the evolution of short periodic binary systems (Toonen et al. 2016). These systems are basically studied by eclipse timing variation (ETV) which tells fundamental information about the outer orbit. The light-travel-time effect (LTTE) that causes

the main variation in the ETV was described by [Irwin \(1952\)](#) in the following form:

$$\Delta_{\text{LTTE}} = -\frac{a_{\text{AB}} \sin i_2}{c} \frac{(1 - e_2^2) \sin(v_2 + \omega_2)}{1 + e_2 \cos v_2}, \quad (1)$$

where  $a_{\text{AB}}$  denotes the semi-major axis of the EB's center of mass around the center of mass of the triple system, while  $i_2$ ,  $e_2$ ,  $\omega_2$  and  $v_2$  stand for the inclination, eccentricity, and argument of periastron of the relative outer orbit and the true anomaly of the third component, respectively. By these orbital parameters, the minimum mass of the third component can also be estimated through the mass function, iteratively, if we know the mass of the eclipsing binary ( $m_{\text{EB}}$ ):

$$f(m_C) = \frac{m_C^3 \sin^3 i_2}{m_{\text{ABC}}^2} = \frac{4\pi^2 a_{\text{AB}}^3 \sin^3 i_2}{GP_2^2}, \quad (2)$$

where  $m_C$  is the mass of the tertiary component and  $m_{\text{ABC}}$  is the total mass of the triple system ( $m_C + m_{\text{EB}}$ ).

In addition to the LTTE, dynamic effects can also be significant which was described in detail in a series of papers by [Borkovits et al. \(2003, 2011, 2015\)](#). However, this only makes a significant contribution in really tight systems. It is typically taken into account when the  $P_2/P_{\text{EB}}$  ratio is 100 or less.

The minimum times can also be affected by other effects like stellar spots (see e.g., [Balaji et al. 2015](#)), apsidal motion ([Gimenez & Garcia-Pelayo 1983](#)) and mass transfer which are not always distinguishable from the light-time effect, especially in case of inadequate sampling.

### 3 DATA PREPARATION AND ANALYSIS

For our investigation we used the CoRoT EB candidate catalog published by [Klagyivik et al. \(2017\)](#) and the unofficial online CoRoT catalogue<sup>1</sup> assembled by J. Devor. From these catalogs we selected those targets which were also observed by TESS multiple times. Figure 1 shows the CoRoT (gray patches) and TESS fields of view in celestial coordinates. From this figure it can be seen that the direction of the galactic anticenter is the area which is covered by TESS sectors 6, 7 and 33, making the identification of triple candidates easier.

In the first step we determined the orbital period of the binaries with Phase Dispersion Minimization (PDM; [Stellingwerf 1978](#)) using the `cuvvarbase`<sup>2</sup> python package. We used the so-called binned linear interpolation method with 100 bin cells. For this purpose we only used the CoRoT light curves.

In the next step we used the TESScut package ([Brasseur et al. 2019](#)) to extract TESS light curves. For each target we downloaded the pixels within a  $5 \times 5$  pixel area around the centroid. To build an aperture we selected only those pixels where the folded light curve had a signal-to-noise ratio (S/N) higher than 1. To always get a light curve, at least the pixel with the highest S/N value was selected. The value of the S/N was calculated from the parameters of the folded and binned light curve, namely the standard deviation of each bin and the amplitude of the binned light curve. To estimate the optimal number of bins, we used the same method as [Bódi & Hajdu \(2021\)](#).

Then, to remove the systematic trends we used the `flatten` method from the `wotan` python package ([Hippke et al. 2019](#)). We

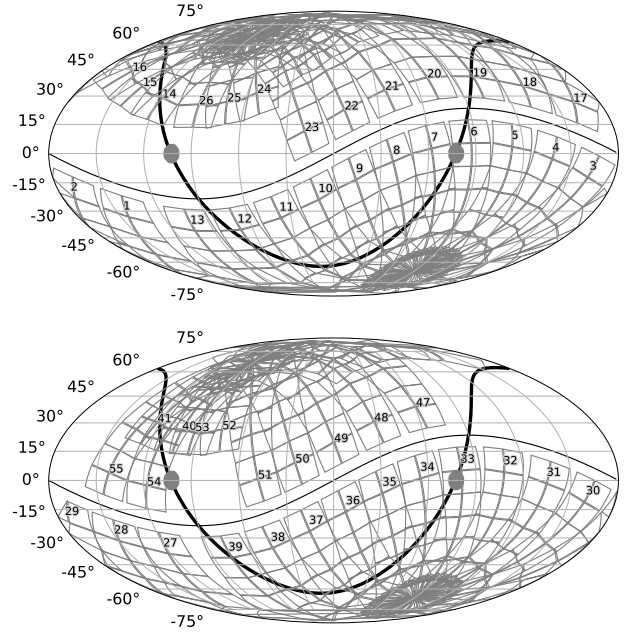


**Figure 1.** The CoRoT (gray patches) and TESS fields of view in celestial coordinates. The numbers are the TESS sectors. The top panel represents the first 2 years of TESS measurements and bottom panel shows the following 2 years. The thick black line is the galactic plane.

set the window length to twice the binary period. Furthermore, we cleared the light curves by removing the outlier points based on the standard deviation of each bin of the folded light curves. Finally, we rescaled the flux values of each observation series so their folded and binned light curves have the same amplitude. This step was necessary to find the correct orbital period of the systems and made it easy to identify systems where the ETV caused dramatic apparent period changes (see e.g., the case of CoRoT 102788679 in section 4).

After this pre-processing, the period was recalculated with the full light curve.

The ETV analysis was performed automatically using the method developed by [Hajdu et al. \(2022\)](#). Then, because of the relatively low number of systems and the poor coverage of the outer orbits, the hierarchical triple candidates were selected manually. We paid special attention to the systems that have been measured more than 3 times, as only under these conditions can the presence of a third body be determined with sufficient certainty. For the others, only the presence of a quadratic trend or apsidal motion could be determined. The manual selection was also supported by the folded light curves, of which some showed significant phase shift.

For the selected candidates the ETV curves were fitted by LTTE, whose parameters were optimized with Levenberg-Marquardt algorithm. In order to get reliable errors we used the Markov chain Monte Carlo (MCMC) method as it is implemented in the `emcee` ([Foreman-Mackey et al. 2013](#)) python package, similarly to [Hajdu et al. \(2022\)](#).

To calculate the minimum mass of the third body, we need to know the total mass of the inner binary. This can be estimated using the period-mass relation of the W UMa-type binaries published by [Dimitrov & Kjurkchieva \(2015\)](#). Based on their paper the mass of the binary is:

$$m_{\text{AB}} = \frac{0.0134}{P^2} \left( -1.154 + 14.633 \cdot P - 10.319 \cdot P^2 \right)^3, \quad (3)$$

<sup>1</sup> [http://www.astro.tau.ac.il/~jdevor/CoRoT\\_catalog/catalog.html](http://www.astro.tau.ac.il/~jdevor/CoRoT_catalog/catalog.html)

<sup>2</sup> <https://github.com/johnh202/cuvvarbase>

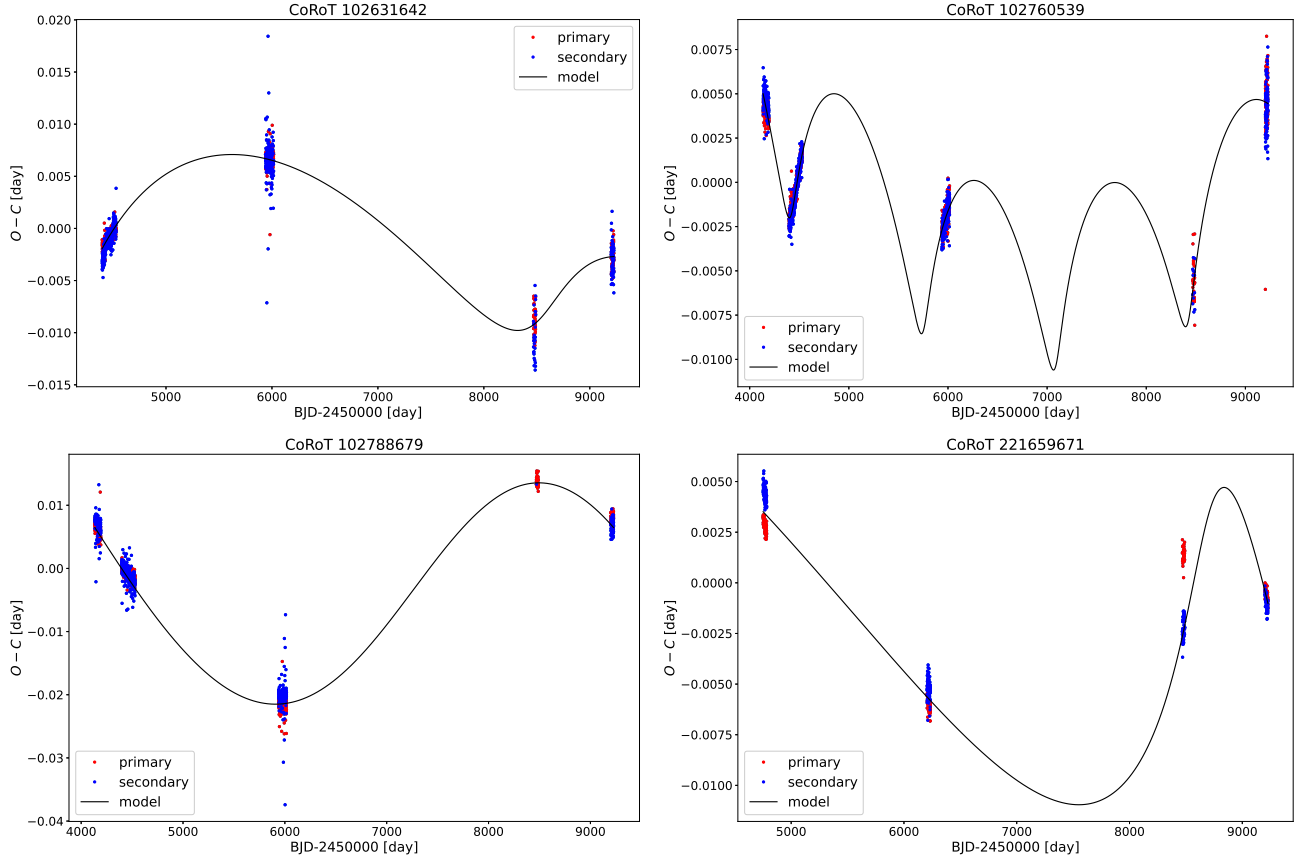


**Figure 2.** ETV of the systems and the best-fitting LTTE models (black curves). The red and blue points correspond to the primary and secondary minima, respectively.

where  $P$  stands for the orbital period of the binary. Using this formula and the equation of the mass function (Eq. 2) we were able to estimate the minimum mass of the third companions.

## 4 RESULTS

We have produced  $O - C$  diagrams for 1428 binary systems, out of which we identified 4 potential hierarchical triple stellar system candidates. The orbital parameters of the systems derived from the LTTE fitting process are listed in Table 1. The  $O - C$  diagrams of the candidates and the best-fitting models are plotted in Figure 2.

Because of the relatively low number of candidates we give some specific details about each of them below.

### CoRoT 102631642

CoRoT 102631642 is our only non-W UMa-type binary system whose mass therefore cannot be determined based on its orbital period. Therefore, we used the usual approximation where the mass of the binary is assumed to be two solar masses. This system is more likely a  $\beta$  Lyr system with the morphology parameter (Prša et al. 2008)  $c = 0.67$ , which was calculated with the package published by Bódi & Hajdu (2021).

The  $O - C$  of the system clearly shows a nearly sinusoidal LTTE (see top left panel of Fig. 2). Nonetheless, the eccentricity of the outer orbit is large, and the fitted orbital parameters have the highest relative errors compared to the other systems in our list.

### CoRoT 102760539

CoRoT 102760539 is the only system that has a relatively short outer period ( $\sim 1300^d$ ) and which could be identified as a triple without the TESS measurements. However, for the proper estimation of the orbital parameters, all measurements – uniquely covering approximately 4 full outer orbits – are necessary. Based on the period-mass correlation of W UMa-type binaries (Dimitrov & Kjurkchieva 2015), the EB’s mass was found to be  $M_{EB} = 1.14 M_{\odot}$ .

### CoRoT 102788679

In most of the triple stellar systems with circular inner orbits the relative ETV ( $dP/P_{EB}$ ) caused by the LTTE is small enough to be unnoticeable in the folded light curve. Only a few exceptions are known, like OGLE-BLG-ECL-253744 (Hajdu et al. 2022) and KIC 9596187 (Borkovits et al. 2016). CoRoT 102788679 is a new member of this group, whose phase-folded light curve is shown in Fig. 3, where we shifted each observation sequence and its LTTE model vertically according to the observation times to create a ‘river plot’, similar to a waterfall diagram (Agol & Fabrycky 2018). The folded light curve of the system also shows detectable O’Connell effect (O’Connell 1951) which is most likely caused by starspots.

Due to the relatively large  $O - C$  amplitude, the PDM method, which was used to determine the orbital period, needed some manual intervention. Otherwise, it would have found a period by which in the folded light curve the two types of minima were interchanged.

**Table 1.** The orbital parameters derived from Levenberg-Marquardt fit and their errors estimated via MCMC sampling.

CoRoT ID	$P_{EB}$ [day]	$t_0$ [BJD-2450000 day]	$a_2 \sin(i_2)$ [ $R_\odot$ ]	$P_2$ [day]	$e_2$	$\tau_2$ [BJD-2450000 day]	$\omega_2$ [deg]	$f (m_c)$ [ $M_\odot$ ]	$M_{min}$ [ $M_\odot$ ]
102631642	0.343116	4397.3067	$304.81^{+247.63}_{-41.26}$	$4567.11^{+996.44}_{-811.71}$	$0.53^{+0.20}_{-0.44}$	$8569.06^{+1297.70}_{-672.27}$	$2.60^{+1.41}_{-0.62}$	$0.02^{+0.13}_{-0.01}$	$0.50^{+0.65}_{-0.10}$
102760539	0.227558	4134.9187	$194.73^{+14.15}_{-11.10}$	$1336.37^{+4.08}_{-4.37}$	$0.66^{+0.05}_{-0.05}$	$4417.27^{+9.23}_{-11.83}$	$2.00^{+0.08}_{-0.10}$	$0.05^{+0.02}_{-0.01}$	$0.54^{+0.05}_{-0.07}$
102788679	0.243944	4134.8952	$741.48^{+580.10}_{-36.06}$	$5773.29^{+1461.34}_{-191.36}$	$0.17^{+0.03}_{-0.13}$	$7316.67^{+713.37}_{-172.31}$	$3.44^{+0.41}_{-0.40}$	$0.16^{+0.39}_{-0.03}$	$0.94^{+0.70}_{-0.09}$
221659671	0.292952	4750.8828	$792.60^{+292.45}_{-113.85}$	$5993.28^{+536.90}_{-320.91}$	$0.55^{+0.01}_{-0.14}$	$8735.43^{+295.72}_{-68.75}$	$3.83^{+0.41}_{-0.16}$	$0.18^{+0.32}_{-0.07}$	$1.16^{+0.73}_{-0.22}$

**Table 2.** Stellar parameters of CoRoT 102788679. The first six values were used to estimate the components' subsurface magnetic field strengths. The last two rows are the results.

Parameter	Value	Notes
$P_{EB}$ [days]	0.243944	
$M_{EB}$ [ $M_\odot$ ]	1.3	Based on Eq. 2.
$a$ [ $R_\odot$ ]	1.5	Based on Kepler's third law.
$M_2/M_1$	0.22	Based on the unofficial catalog.
$R_1/a$	0.313	Based on the unofficial catalog.
$R_2/a$	0.3949	Based on the unofficial catalog.
$B_1$ [kG]	129.1	
$B_2$ [kG]	15.3	

The  $O - C$  shows the most sinusoidal-shaped LTTE among our targets, which is strengthened by the fitted small eccentricity value.

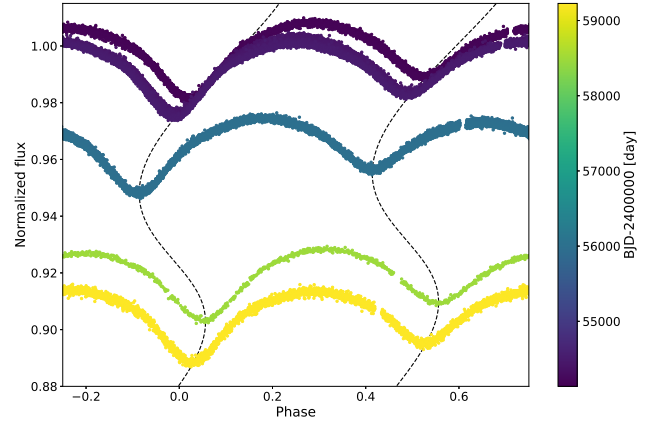
In this type of active stars the angular momentum can also be disturbed by a magnetic torque which causes a nearly sinusoidal ETV. This effect is the so called Applegate mechanism (Applegate 1992) which may play a role in formation and evolution of close binaries. There are many papers which describe how the stellar parameters affect the period and the amplitude of the mechanism (Lanza et al. 1998; Völschow et al. 2018) which may help to strengthen or disprove the presence of this effect.

We used the following formula to estimate the strength of the magnetic field (Mitnyan et al. 2018):

$$B^2 \sim 10 \frac{GM^2}{R^4} \left(\frac{a}{R}\right)^2 \frac{\Delta P}{P_{mod}}, \quad (4)$$

where  $B$  is the strength of the magnetic field,  $M$  and  $R$  are the mass and the radius of a given component, respectively,  $a$  is the semi-major axis,  $\Delta P$  is the amplitude of the  $O - C$  diagram and  $P_{mod}$  is the period of the modulation.

From the period-mass correlation, this binary system's mass was calculated to be  $M_{EB} = 1.3M_\odot$ . Based on the Kepler's third law the semimajor axis is  $a \sim 1.5R_\odot$ . Also, using the relative parameters from the unofficial catalog of CoRoT binaries<sup>3</sup> we estimated the possible strength of the subsurface magnetic fields of both components separately. The parameters used to calculate the magnetic fields and the results are listed in Table 2. Based on these, if the secondary component has a magnetic field specified in the table, then the Applegate mechanism cannot be completely excluded from the possible causes of the period change. Similar example can be found in the case of VW Cep (Mitnyan et al. 2018).

**Figure 3.** River plot of the folded light curve of CoRoT 102788679. For better visibility we shifted each observation sequence and the LTTE model (dashed lines) vertically as a function of the observation time, which is depicted by the color bar.

#### CoRoT 221659671

This is the only system from our candidates where the light curve is significantly influenced by stellar spots. These spots also significantly affect the shape of the  $O - C$  diagram, which can easily mislead the 'normal' LTTE fitting process, especially if there is a large difference between the number of the data points in the two kinds of minima (primary and secondary). Therefore, for this system we calculated the average  $O - C$  diagram, which not only smoothed out the effect of the spots, but also significantly reduced the number of data points to be fitted, which made the fitting process faster.

The fitted LTTE variation yielded the longest outer period – about 6000 days – among our targets. The mass of the binary was estimated to be  $M_{EB} = 1.8M_\odot$ .

#### 4.1 Period-period distribution

In Fig. 4 we show the period-period ( $P_1 - P_2$ ) distribution of triple systems, for which we used the data from several papers for comparison (Borkovits et al. 2016, 2022; Zasche et al. 2016, 2017; Hajdu et al. 2017, 2019, 2022; Rappaport et al. 2022; Hong et al. 2022). The red dots with error bars are the four new CoRoT-TESS triple candidates. With the exception of CoRoT 102760539, all other candidates have longer outer periods than most triple systems and are on the edge of the clustering seen in OGLE systems. It can also be seen that the four new systems have longer outer period than any

<sup>3</sup> [http://www.astro.tau.ac.il/~jdebor/CoRoT\\_catalog/catalog.html](http://www.astro.tau.ac.il/~jdebor/CoRoT_catalog/catalog.html) other CoRoT or TESS target.



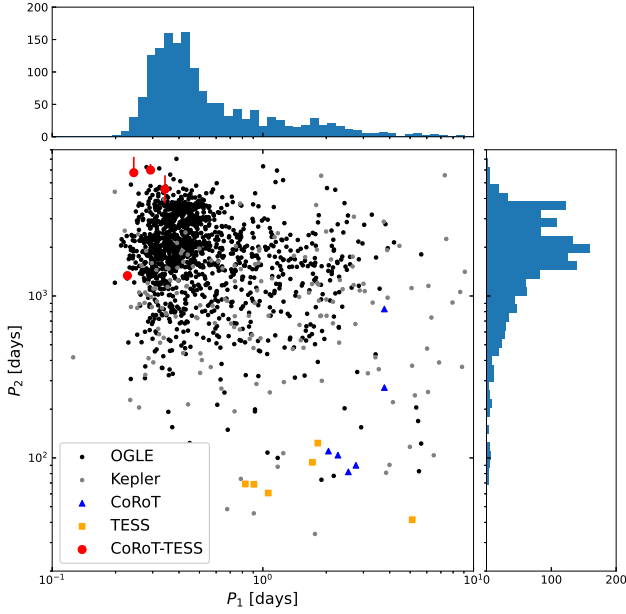


**Figure 4.** Period-period ( $P_1 - P_2$ ) diagram of triple systems. The black and gray points represent the OGLE (Zasche et al. 2016, 2017; Hajdu et al. 2019, 2022; Hong et al. 2022) and the *Kepler* (Borkovits et al. 2016) triples, respectively, while the blue triangles and the orange squares stand for the *CoRoT* (Hajdu et al. 2017) and *TESS* (Borkovits et al. 2022; Rappaport et al. 2022) hierarchical triple candidates, respectively. The red circles with the errorbars represent the four new *CoRoT-TESS* triple stellar candidates.

**Table 3.** Further systems with significant ETV. The full list is available as online supplementary material.

ID	$P_{EB}$ [day]	$T_0$ [BJD-2450000 day]	Type of variability
102285983	3.483354	5108.164850	parabolic ETV
102383485	7.830361	5101.539991	apsidal motion
102568782	0.589398	4397.000981	parabolic ETV
102573289	2.111683	4395.621930	apsidal motion
102574112	3.376890	4396.478732	apsidal motion
...			

#### 4.2 Systems with significant ETV

During our manual search for triple stellar candidates we also found several other systems which show significant, but not strictly periodic ETVs. These systems and their basic parameters, the orbital period and epoch of the binary, and the type of the variation visible in their  $O - C$  diagrams, are listed in Table 3. The full version of the table is available online. Based on the observed changes in the  $O - C$  diagram, 2 groups can be distinguished.

In the first group there are systems whose ETV shows parabolic trend which may be caused by mass transfer. However, we cannot rule out the possibility of the effect of a third body, but since we do not have enough observations, this cannot be decided.

The second group contains systems whose  $O - C$  diagrams show intercepting lines, which is the typical manifestation of apsidal motion. In some cases, the variation is also visible in the folded light curve, as well. A good example is *CoRoT* 110743209, whose folded

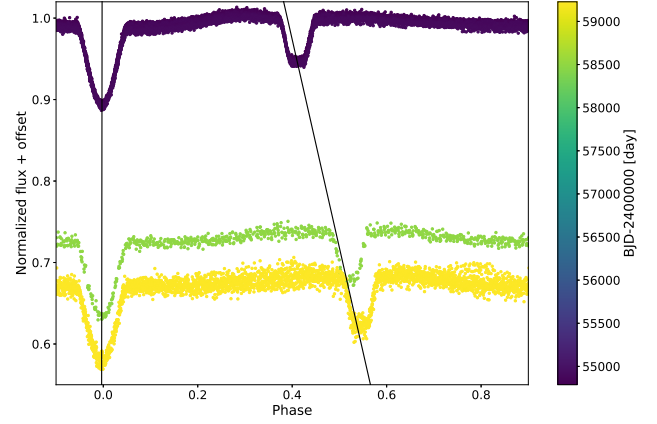


**Figure 5.** River plot of the folded light curve of *CoRoT* 110743209, where each observation sequence is shifted vertically according to its observation time. The solid black lines are only shown to highlight the variation of the eclipse midpoints.

light curve is plotted in Figure 5 and the primary minima are shifted to zero phase to highlight the variation in the secondary minima.

## 5 SUMMARY AND CONCLUSIONS

In this paper we report the results of a search for triple stellar candidates, which were observed by both the *CoRoT* and *TESS* space telescopes. To maximize the possibly of finding such systems, we pre-selected a list of targets that were observed in multiple *TESS* sectors. Out of about one and half thousand binary systems, we identified 4 new hierarchical triple candidates, whose eclipse timing variations (ETV) can be fitted with light-travel-time effect (LTTE). This number doubles the number of known *CoRoT* triples.

In case of each triple stellar system candidate, we determined and listed the periods of the inner binaries and the orbital parameters of the tertiary, along with its estimated mass. In three cases, only the *TESS* observations made it possible to discover the tertiary candidate. In one case, where the light curve also shows significant phase shift, the *CoRoT* observations were enough to reveal the variability, but they were not enough to determine the proper orbital parameters. This shows that the combination of different observation sequences made by different telescopes holds great potential for the study of multiple stellar systems.

Besides the triples, we also listed systems that show significant ETV, probably due to mass transfer between the components or apsidal motion, which could be the subject of a further research, possibly supplemented with ground-based follow-up observations.

## ACKNOWLEDGEMENTS

This paper includes data collected by the *TESS* mission. Funding for the *TESS* mission is provided by the NASA Science Mission Directorate. The *CoRoT* space mission was developed and operated by CNES, with contributions from Austria, Belgium, Brazil, ESA, Germany, and Spain. This project has been supported by the NKFIH-OTKA grant KH-130372 and the KKP-137523 ‘SeismoLab’ Élvonal grant of the Hungarian Research, Development and Innovation Office, by the Lendület Program of the Hungarian Academy of Sciences, project No. LP2018-7/2021, and by the MW-Gaia COST

Action (CA18104). This research has made use of NASA's Astrophysics Data System.

## DATA AVAILABILITY

The original CoRoT light curves are available at Vizier<sup>4</sup>. The full table of systems with significant ETV is available online as an external material. The derived data generated in this research will be shared on [https://konkoly.hu/KIK/data\\_en.html](https://konkoly.hu/KIK/data_en.html) web page.

## REFERENCES

- Agol E., Fabrycky D. C., 2018, in Deeg H. J., Belmonte J. A., eds., *Handbook of Exoplanets*. p. 7, doi:10.1007/978-3-319-55333-7\_7
- Alencar S. H. P., et al., 2010, *A&A*, **519**, A88
- Applegate J. H., 1992, *ApJ*, **385**, 621
- Auvergne M., et al., 2009, *A&A*, **506**, A41
- Balaji B., Croll B., Levine A. M., Rappaport S., 2015, *MNRAS*, **448**, 429
- Bódi A., Hajdu T., 2021, *ApJS*, **255**, 1
- Borkovits T., Érdi B., Forgács-Dajka E., Kovács T., 2003, *A&A*, **398**, 1091
- Borkovits T., Csizmadia S., Forgács-Dajka E., Hegedüs T., 2011, *A&A*, **528**, A53
- Borkovits T., Rappaport S., Hajdu T., Sztakovics J., 2015, *MNRAS*, **448**, 946
- Borkovits T., Hajdu T., Sztakovics J., Rappaport S., Levine A., Bíró I. B., Klagyivik P., 2016, *MNRAS*, **455**
- Borkovits T., et al., 2022, *MNRAS*, **510**, 1352
- Brasseur C. E., Phillip C., Fleming S. W., Mullally S. E., White R. L., 2019, *Astrocute: Tools for creating cutouts of TESS images* (ascl:1905.007)
- Chiappini C., et al., 2015, *A&A*, **576**, L12
- Conroy K. E., Prša A., Stassun K. G., Orosz J. A., Fabrycky D. C., Welsh W. F., 2014, *AJ*, **147**, 45
- Dimitrov D. P., Kjurkchieva D. P., 2015, *MNRAS*, **448**
- Foreman-Mackey D., Hogg D. W., Lang D., Goodman J., 2013, *PASP*, **125**, 306
- Gimenez A., Garcia-Pelayo J. M., 1983, *Ap&SS*, **92**, 203
- Hajdu T., Borkovits T., Forgács-Dajka E., Sztakovics J., Marschalló G., Benkő J. M., Klagyivik P., Sallai M. J., 2017, *MNRAS*, **471**, 1230
- Hajdu T., Borkovits T., Forgács-Dajka E., Sztakovics J., Marschalló G., Kutrovátz G., 2019, *MNRAS*, **485**
- Hajdu T., Borkovits T., Forgács-Dajka E., Sztakovics J., Bódi A., 2022, *MNRAS*, **509**, 246
- Hipke M., David T. J., Mulders G. D., Heller R., 2019, *AJ*, **158**, 143
- Hong K., Woo Lee J., Park J.-H., Kim H.-Y., Lee C.-U., Kim H.-W., Kim D.-J., Han C., 2022, *AJ*, **163**, 157
- Irwin J. B., 1952, *ApJ*, **116**, 211
- Klagyivik P., Deeg H. J., Cabrera J., Csizmadia S., Almenara J. M., 2017, *A&A*, **602**, A117
- Lanza A. F., Rodono M., Rosner R., 1998, *MNRAS*, **296**, 893
- Lanza A. F., et al., 2009, *A&A*, **493**, 193
- Léger A., et al., 2009, *A&A*, **506**, 287
- McGinnis P. T., et al., 2015, *A&A*, **577**, A11
- Mitnyan T., et al., 2018, *A&A*, **612**, A91
- Mitnyan T., Borkovits T., Rappaport S. A., Pál A., Maxted P. F. L., 2020, *MNRAS*, **498**, 6034
- Mitnyan T., Borkovits T., Pál A., Hajdu T., 2021, in *Posters from the TESS Science Conference II (TSC2)*. p. 127, doi:10.5281/zenodo.5130636
- Naoz S., Fabrycky D. C., 2014, *ApJ*, **793**, 137
- O'Connell D. J. K., 1951, *Publications of the Riverview College Observatory*, **2**, 85
- Prša A., Guinan E. F., Devinney E. J., DeGeorge M., Bradstreet D. H., Giammarco J. M., Alcock C. R., Engle S. G., 2008, *ApJ*, **687**, 542
- Rappaport S. A., et al., 2022, *MNRAS*
- Ricker G. R., et al., 2015, *Journal of Astronomical Telescopes, Instruments, and Systems*, **1**, 014003
- Shappee B. J., Thompson T. A., 2013, *ApJ*, **766**, 64
- Stellingwerf R. F., 1978, *ApJ*, **224**, 953
- Toonen S., Hamers A., Portegies Zwart S., 2016, *Computational Astrophysics and Cosmology*, **3**
- Völschow M., Schleicher D. R. G., Banerjee R., Schmitt J. H. M. M., 2018, *A&A*, **620**, A42
- Zasche P., Wolf M., Vraštil J., Pilarčík L., Juryšek J., 2016, *A&A*, **590**, A85
- Zasche P., Wolf M., Vraštil J., 2017, *MNRAS*, **469**, 2952

This paper has been typeset from a  $\text{\LaTeX}$  file prepared by the author.

<sup>4</sup> <https://vizier.cds.unistra.fr/viz-bin/VizieR-3?-source=B/corot>